Two-Degrees of Freedom and Variable Structure Controllers for Induction Motor Drives

Mohamed ZAKY[1,2*], Ezzeddine TOUTI[1,3], Haitham AZAZI[2]
[1]*Department of Electrical Engineering, Northern Border University, Arar,1321, Saudi Arabia*
[2]*Department of Electrical Engineering, Minoufiya University, Shebin El-Kom, 32511, Egypt*
[3]*Department of Electrical Engineering, Tunis University, Montfleury, 1008, Tunisia*
[*]*mszaky78@yahoo.com*

Abstract—**This paper presents a two-degrees-of-Freedom (2DOF) and variable structure control (VSC) schemes for induction motor (IM) drives. The designed VSC incorporates independent feedback and feedforward terms as 2DOF control principle. This structure improves the response of the proposed VSC under speed reference tracking and load disturbance changes. Stability of VSC using Lyapunov theory is discussed. Due to the variable nature of the switching function of VSC, two conditions to ensure Lyapunov stability candidate are derived based on the error signal. A design criterion for the parameters of VSC are introduced to guarantee the stability. The complete IM drive system with the proposed VSC controller is built using MATLAB/Simulink. A laboratory prototype is executed experimentally using DSP-DS1104 control board. All controllers are implemented practically. Simulation and experimental results are provided under different working conditions. Performance evaluation of classic control schemes and the proposed VSC approach is presented. The proposed VSC approach gives superior behavior under speed reference variations and torque disturbances. The disturbances using the proposed controller are strongly suppressed compared to classic 2DOF control scheme.**

Index Terms—**induction motor drives, field oriented control, 1DOF controller, 2DOF controller, variable structure control.**

I. INTRODUCTION

AC drives have been commonly employed in motion control industrial applications. Induction motors (IMs) with a field oriented control have been considered one of the high behavior AC drives. They are characterized by robustness, low cost, low maintenance, and ruggedness. Different applications of electrical drives require high ranking requirements of the controller. Applications such as compressors, press machines, and robot manipulator require a constant speed of the IMs under load torque disturbances and uncertainties. Also, an accurate movement in a robot arm drive under a variation of moment of inertia is of a considerable importance [1]-[2]. The industrial applications of AC servo drives using two-degrees-of-freedom (2DOF) control are robotics, conveyor belts, printing presses/printers, textiles, antenna positioning, metal cutting and metal forming machines

Field oriented control theory has improved the control properties of the AC machines to be as a separately excited DC motors. IMs under this control strategy are capable of controlling the position and the speed precisely. So, the IMs are a good choice for AC servo drives that commonly employed in motion control industrial applications [1]-[3]. In [1], design and analysis of 2DOF controller for split stator IM were executed and the electromagnetic parameters were determined. The finite element model in three dimensional (3-D) analysis of electromagnetic field was utilized of 2DOF direct drive IM [2]. Speed control of 2DOF IM with helical rotor was combined with the stator of three-phase rotary IM to realize the required motion type [3]. The fault ride through (FRT) in double fed induction generator wind turbine was improved based on 2DOF with internal model control. This controller takes into consideration the power limit of back to back converters [4]. The design and analysis of one-degree-of-freedom (1DOF) and 2DOF controllers for IM were addressed in [5]. In [6], the speed controller of permanent magnet synchronous machine was executed using proportional integral (PI) controller with 2DOF. To perform the accurate determination of the displacement along two axes in 2DOF of piezoelectric actuator, the measurement was taken based on self-sensing technique [7].

Many electrical drives use a traditional 1DOF controller [8-10]. It is characterized by simplicity and straightforward in its design and implementation. However, it has only a feedback control loop. Thus, it is difficult to maintain the desired performance under reference changes, parameters uncertainty, and load fluctuations. Alternatively, 2DOF controller is a well-recognized technique to simultaneously control the tracking commands and load disturbances [5], [11]. This control approach is constructed from feedback and feed-forward control loops which are separately designed [5]. Nevertheless, the gains of 2DOF control method depend on its load values and machine parameters. Consequently, the change of machine parameters, modeling errors, and load fluctuations degrade the desired specifications of the 2DOF controller. Therefore, the vital robustness and tracking performances may not be precisely guaranteed [12]-[14]. Sensorless speed control in the whole speed range based on high frequency injection with 2DOF current control for PMSM was addressed in [15]. A comparison between self-tuned PI approach and conventional 1DOF, and 2DOF PI controller fed hybrid stepper motor (HSM) drive was presented in [16]. The parameters for self-tuned PI approach were adopted. Classic control schemes using 1DOF, 2DOF, and self-tuning PI controller were presented in [17] and compared with a chatter free variable structure controller (VSC) fed HSM. A

The authors gratefully acknowledge the approval and the support of this research study by the grant no. ENG-2017-1-7-F-7027 from the Deanship of Scientific Research at Northern Border University, Arar, KSA.

Digital Object Identifier 10.4316/AECE.2018.01009

PI controller with a load torque estimator was presented in [18] to improve the load torque disturbance rejection.

A disturbance observer-based control scheme for integral processes with dead-time was applied in [19]. This approach is 2DOF internal model control. It separates the disturbance response from the set point response. PI and PID parametric conditions were derived in [20] for both robust stability and the controller robustness of plants employed in integral-type servo systems. 2DOF control approach using PID controller and filter for integrating processes with time delay was presented in [21]. The gains of the PID controller were selected using Linear Quadratic Regulator (LQR) with dominant pole placement approach.

VSC approach is characterized by its capability to change its output according to the value of its input. A robust VSC approach with an adaptive sliding gain to minimize the chattering was introduced in [22]. VSC is considered a robust to disturbances and uncertainties due to modeling and parameters [23]-[26].

Recently, sliding mode control (SMC) has been applied for different applications. In [27], SMC was used to alleviate the nonlinear behavior of the hysteresis comparator for boost converters. An optimized SMC was proposed in [28] for single-phase dynamic voltage restorers. This can be achieved by designing the sliding gain to enlarge the existence region to maximize the sliding mode. SMC with a combined switched/time-based adaptation strategy was proposed in [29]. It was applied for highly uncertain nonlinear systems using the single-link manipulator with flexible joint and negligible damping. This allows for an online adaptation of the control effort with the actual magnitude of the uncertain terms. Two model-free SMC structures were suggested in [30] and compared with a model-free intelligent proportional-integral control system structure. They applied on a nonlinear laboratory twin rotor aerodynamic system for validation purposes. Integral VSC was introduced in [31] for brushless direct-drive motor.

This paper proposes the following new contributions in comparison to the state-of-the-art works:

a) VSC is designed as the 2DOF control structure.
b) The stability of VSC using Lyapunov theory is guaranteed.
c) The conditions to ensure Lyapunov stability candidate are derived based on the error signal.
d) Unlike [17], a design criterion for the parameters of the proposed VSC controller is provided.
e) A fair comparison between the proposed VSC structure and the classic 1DOF and 2DOF control methods is offered.
f) The validation of the proposed VSC approach is done by simulations and experiments for the IM drive employing DSP-DS1104 platform.

The new contributions guarantee the following advantages compared to classic control methods (1DOF and 2DOF) that presented in [32]:

1) The tracking performance of the IM drive is significantly improved.
2) The disturbances and uncertainties using the proposed controller are strongly suppressed.

This paper is organized as follows: mathematical models of the vector control and IM are presented in the next section. Section III introduces traditional 1DOF and 2DOF control schemes. Section IV focuses on the design of the proposed VSC approach. Stability of VSC using Lyapunov theory and the selection of the controller parameters is presented in Section V. In Section VI, the simulation and experimental results are presented and discussed. The comparison tests are provided in Section VII. The conclusions are given in Section VIII.

II. Mathematical Models of the Vector Control and IM

A. IM Model

The IM is described in a stationary reference frame using (1) and (2).

$$\frac{di_s^s}{dt} = \frac{1}{\sigma L_s}\left(v_s^s - R_s i_s^s - \frac{L_m}{L_r}\frac{d\lambda_r^s}{dt}\right) \tag{1}$$

$$\frac{d\lambda_r^s}{dt} = \frac{L_m}{T_r} i_s^s - \left(\frac{1}{T_r} - J\omega_r\right)\lambda_r^s \tag{2}$$

where,

v_s^s	is the stator voltage vector,
i_s^s	is the stator current vector,
λ_r^s	is the rotor flux vector,
R_s	is the stator resistance,
R_r	is the rotor resistance,
L_m	is the magnetizing inductance,
L_r	is the rotor leakage inductance,
L_s	is the stator leakage inductance,
ω_r	is the rotor speed,
$\sigma = 1 - \frac{L_m^2}{L_s L_r}$	is the leakage coefficient, and
$T_r = \frac{L_r}{R_r}$	is the rotor time constant.

The electromechanical equation is given by;

$$T_e = J\frac{d\omega_r}{dt} + B\omega_r + T_L \tag{3}$$

The electromagnetic torque is expressed as;

$$T_e = \frac{2}{3}\cdot\frac{P}{2}\cdot\frac{L_m}{L_r}\left[i_{qs}^s\lambda_{dr}^s - i_{ds}^s\lambda_{qr}^s\right] \tag{4}$$

where,

T_e	is the motor torque
T_L	is the load torque
J	is moment of inertia,
B	is the friction coefficient,
P	is the number of poles,

i_{qs}^{s} is the q-axis stator current

i_{ds}^{s} is the d-axis stator current

λ_{qr}^{s} is the q-axis rotor flux

λ_{dr}^{s} is the d-axis rotor flux

B. Indirect Field Oriented Control System

The Indirect Field Oriented Control (IFOC) for IM is depicted in Fig. 1. The speed controller compares the reference speed ω_r^* and actual speed ω_r to give the desired performance during the speed reference tracking and the load torque disturbances. The output of the speed controller gives the torque command T_e^* that uses to obtain the quadrature current i_{qs}^* using (5).

$$i_{qs}^* = \frac{2}{3}\cdot\frac{2}{P}\cdot\frac{L_r}{L_m}\cdot\frac{T_e^*}{\lambda_r^*} \tag{5}$$

The direct current i_{ds}^* can be computed from the rotor flux λ_r^* as given in (6).

$$i_{ds}^* = \frac{\lambda_r^*}{L_m} \tag{6}$$

The IFOC strategy calculates the angle θ_e which is needed for axis transformation using ω_r and the slip speed ω_{sl} as obtained in (7).

$$\theta_e = \int(\omega_r + \omega_{sl})dt \tag{7}$$

To compute the slip speed ω_{sl}, the quadrature current i_{qs}^* and the motor parameters are employed based on (8).

$$\omega_{sl} = \frac{L_m}{\lambda_r^*}\cdot\frac{R_r}{L_r} i_{qs}^* \tag{8}$$

The $\left(i_{qs}^*,\ i_{ds}^*\right)$ in the synchronously reference frame as DC components are transformed to $\left(i_{qs}^{s*},\ i_{ds}^{s*}\right)$ in the stationary reference frame as AC orthogonal components using the angle θ_e as described in (9).

$$\left.\begin{aligned} i_{qs}^{s*} &= i_{qs}^*\cos\theta_e + i_{ds}^*\sin\theta_e \\ i_{ds}^{s*} &= -i_{qs}^*\sin\theta_e + i_{ds}^*\cos\theta_e \end{aligned}\right\} \tag{9}$$

The three-phase reference currents $(i_a^*,\ i_b^*,\ i_c^*)$ are computed from the $\left(i_{qs}^{s*},\ i_{ds}^{s*}\right)$ based on (10).

$$\left.\begin{aligned} i_a^* &= i_{qs}^{s*} \\ i_b^* &= -\frac{1}{2}i_{qs}^{s*} - \frac{\sqrt{3}}{2}i_{ds}^{s*} \\ i_c^* &= -\frac{1}{2}i_{qs}^{s*} + \frac{\sqrt{3}}{2}i_{ds}^{s*} \end{aligned}\right\} \tag{10}$$

The current controllers which composed of three hysteresis regulators compare the actual and reference currents to construct the gate pulses of the PWM inverter as demonstrated in Fig. 2.

III. Traditional Control Schemes

To confirm the efficacy of the proposed VSC scheme, traditional 1DOF and 2DOF control schemes are used for the performance comparison. A detailed investigation of traditional 1DOF and 2DOF approaches was introduced in [32].

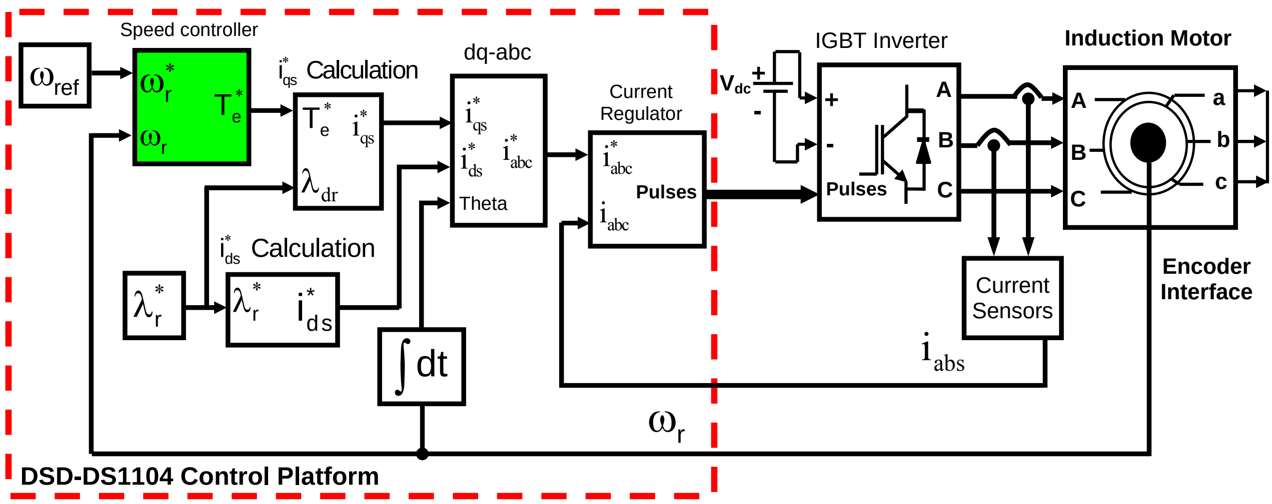

Figure 1. Structure of the complete IFOC of speed control for IM drive

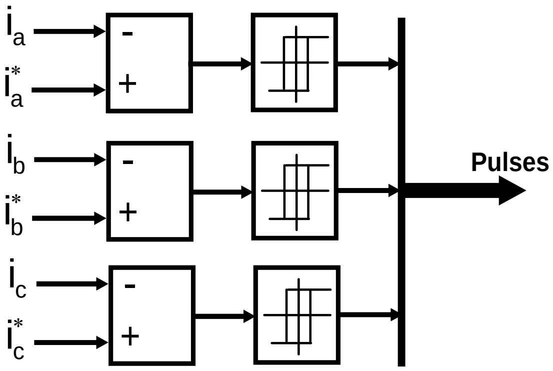

Figure 2. Hysteresis controllers for producing gate pulses

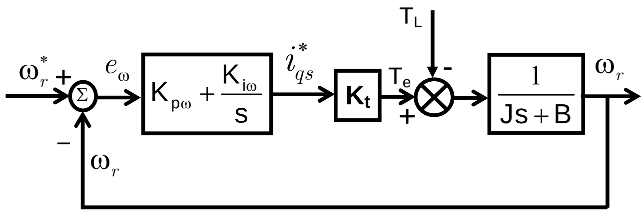

Figure 3. Schematic block diagram for 1DOF controller of the IM

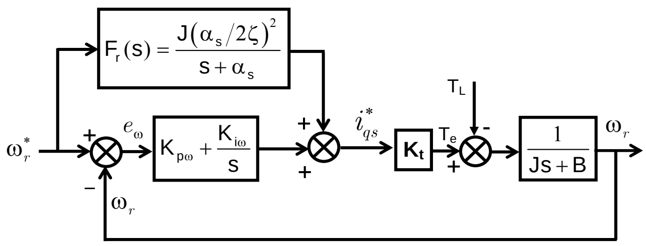

Figure 4. Schematic block diagram for 2DOF controller of the IM

A. Traditional 1DOF Control Scheme

The traditional 1DOF schematic diagram of the IM drive is shown in Fig. 3. The output of the 1DOF is described using (11).

$$\left.\begin{aligned} \frac{i_{qs}^*(s)}{e_\omega(s)} &= K_{p\omega} + \frac{K_{i\omega}}{s} \\ e_\omega(s) &= \omega_r^*(s) - \omega_r(s) \end{aligned}\right\} \tag{11}$$

where,

$K_{p\omega}$ is the proportional gain of the 1DOF controller, and

$K_{i\omega}$ is the integral gain of the 1DOF controller.

These gains are selected as in [32] for the performance comparison.

B. Traditional 2DOF Control Scheme

The traditional 2DOF schematic diagram of the IM drive is demonstrated in Fig. 4. The output of the 2DOF controller can be described as follows [32],

$$i_{qs}^* = F(s) + F_r(s) \tag{12}$$

$$F(s) = K_{p\omega} + \frac{K_{i\omega}}{s} \tag{13}$$

$$F_r(s) = \frac{J\left(\alpha_s/2\zeta\right)^2}{s+\alpha_s} \tag{14}$$

where,

α_s is the bandwidth of the drive transfer function, and

ζ is the relative damping.

IV. Proposed VSC Approach

The equation (15) is used to derive the VSC algorithm.

$$\dot{\omega}_r(t) = a\omega_r(t) + bi_q^*(t) + fT_L \tag{15}$$

where,

$e(t) = \omega_r^*(t) - \omega_r(t)$,

$a = \frac{-B}{J},\ b = \frac{K_m}{J},\ f = -\frac{1}{J}$

and $\omega_r^*(t)$ represents command speed.

Speed error derivative offers

$$\dot{e}(t) = \dot{\omega}_r^*(t) - \dot{\omega}_r(t) \tag{16}$$

Using (15) and substitute in (16) provides,

$$\dot{e}(t) = \dot{\omega}_r^*(t) - a\omega_r(t) - bi_{qs}^*(t) - fT_L \tag{17}$$

This equation is rewritten by

$$\dot{e}(t) = ae(t) + bu_{eq}(t) - fT_L \tag{18}$$

The variable $u_{eq}(t)$ can be expressed as,

$$u_{eq}(t) = -i_{qs}^*(t) - \frac{a}{b}\omega_r^*(t) + \frac{1}{b}\dot{\omega}_r^*(t) \tag{19}$$

The VSC scheme is designed by select the following switching manifold as [17], [31].

$$S(t) = e(t) + (a+bk)\int_0^t e(\tau)d\tau = 0 \qquad k > 0 \tag{20}$$

The control law of VSC is calculated using (21).

$$u_{eq}(t) = ke(t) - \lambda\,\text{sgn}(S(t)) \tag{21}$$

The parameter λ is selected to represent the limit of the uncertainties and disturbances.

The $\text{sgn}(S)$ represents the relay action and expressed as.

$$\text{sgn}(S(t)) = \begin{cases} +1, & if \quad \text{S(t)} > 0 \\ -1, & if \quad \text{S(t)} < 0 \end{cases} \tag{22}$$

The reference current i_{qs}^* is designed using (19) and (21) as follows,

$$i_{qs}^*(t) = -ke(t) + \lambda\,\text{sgn}(S(t)) - \frac{a}{b}\omega_r^*(t) + \frac{1}{b}\dot{\omega}_r^*(t) \tag{23}$$

Equation (23) is considered the output of the VSC scheme [17]. When reconstruct (23) to be in the form of 2DOF control structure, the following feedback and feed-forward terms are introduced. This new structure of the proposed VSC scheme is shown in Fig. 5.

$$i_{qs}^*(t) = F_e(t) + F_{f\omega}(t) \tag{24}$$

$F_{fw}(s)$ represents the feedforward term of the new VSC speed controller and it is defined as,

$$F_{f\omega}(t) = -\frac{a}{b}\omega_r^*(t) + \frac{1}{b}\dot{\omega}_r^*(t) \tag{25}$$

$F_e(s)$ represents the feedback term of the new VSC speed controller and it is defined as,

$$F_e(t) = -ke(t) + \lambda\,\mathrm{sgn}(S(t)) \tag{26}$$

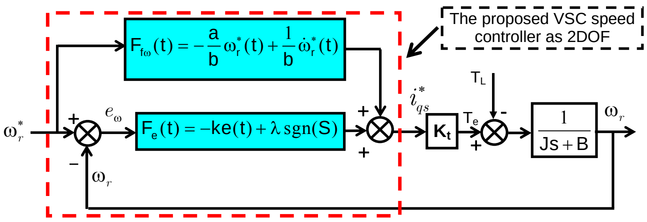

Figure 5. Schematic block diagram for the proposed VSC approach of the IM as 2DOF structure

(B) Sliding Mode Condition

During the sliding mode phase of the VSC, the switching manifold becomes:

$$S(t) = \dot{S}(t) = 0 \tag{27}$$

Then, the switching variable dynamics from (20) provides:

$$\dot{S}(t) = \dot{e}(t) + (a + bk)e(t) = 0 \tag{28}$$

The solution of (28) can be obtained by

$$\dot{e}(t) = -(a + bk)e(t) \tag{29}$$

Equation (29) indicates that the speed error *e(t)* converges to zero in the steady state. The time of convergence relies mainly on the selection of the gain *k*.

V. Stability of VSC

To guarantee the stability of the VSC, Lyapunov function candidate is defined as follows:

$$V(t) = \frac{1}{2}S^2(t) \tag{30}$$

The sufficient condition of stability using Lyapunov stability theory is satisfied if the inequality of (31) is realized.

$$\dot{V}(t) < 0 \tag{31}$$

Then,

$$\dot{V}(t) = S(t)\dot{S}(t) < 0 \tag{32}$$

which is used to design the VSC parameters that ensures the stability.

From (20), the derivative of the switching manifold is:

$$\dot{S}(t) = \dot{e}(t) + (a + bk)e(t) \tag{33}$$

Using (18) and substituting in (33), $\dot{S}(t)$ becomes

$$\dot{S}(t) = ae(t) + bu_{eq}(t) - fT_L + (a + bk)e(t) \tag{34}$$

Introduce (21) in (34), then $\dot{S}(t)$ gives

$$\begin{aligned}\dot{S}(t) &= ae(t) + b\left(ke(t) - \lambda\,\mathrm{sgn}(S(t))\right) - fT_L + (a + bk)e(t)\\ &= (2a + 2bk)e(t) - b\lambda\,\mathrm{sgn}(S(t)) - fT_L\end{aligned} \tag{35}$$

Substituting (35) in (32), the expression of $\dot{V}(t)$ gives

$$\begin{aligned}\dot{V}(t) &= S(t)\dot{S}(t)\\ &= S(t)\left((2a + 2bk)e(t) - b\lambda\,\mathrm{sgn}(S(t)) - fT_L\right) < 0\end{aligned} \tag{36}$$

Then, the existence conditions of VSC can be designed. Two possible conditions are derived according to the value of $S(t)$.

Case 1: $|S(t)| > 0 \Rightarrow \mathrm{sgn}\left(S(t)\right) = +1$:

Substitute in (36), the condition for stability becomes:

$$\left((2a + 2bk)e(t) - b\lambda - fT_L\right) < 0 \tag{37}$$

Then, λ can be derived as:

$$\lambda > \frac{\left((2a + 2bk)e(t) - fT_L\right)}{b} \tag{38}$$

Case 2: $|S(t)| < 0 \Rightarrow \mathrm{sgn}\left(S(t)\right) = -1$:

Introduce in (36), the condition for stability gives:

$$\left((2a + 2bk)e(t) + b\lambda - fT_L\right) > 0 \tag{39}$$

Then, λ can be derived as:

$$\lambda > -\frac{\left((2a + 2bk)e(t) - fT_L\right)}{b} \tag{40}$$

The value of λ that satisfies the two conditions is:

$$\lambda > \left|\frac{\left((2a + 2bk)e(t) - fT_L\right)}{b}\right|$$

To design the proposed VSC, the next steps are followed as:

- Select the parameters of VSC: $\lambda = 55$, $L = 0.01$, $k = 0.5$.
- Calculate the parameters *a* and *b* from the IM parameters.
- Set the parameters of 2DOF: $\alpha_s = 50$ rad/sec and ζ = 0.61.
- Apply the block diagram of Fig. (5) using (23) to calculate the reference current i_{qs}^*.

VI. Results and Discussion

A. Laboratory Drive Setup

Laboratory implementation of the IFOC of the IM is carried out with the traditional 1DOF and 2DOF approaches as well as the proposed VSC approach. Fig. 6 demonstrates the experimental layout for IM drive system using DSP-

DS1104 control platform. The structure of IM drive consists of 1.1 kW IM integrated to DC generator for loading purposes, PWM IGBT's inverter, gate drive and interface circuits, incremental encoder for speed measuring, current sensors for current measuring, and a DS11104 control board. The MATLAB/Simulink is employed for model built. The DSP platform uses a dSPACE-DS1104.

The actual speed is measured using 2048 PPR encoder for speed control of the IM. The measured speed is compared to a speed command. The error is treated using the speed controller to give the suitable torque command. Then, the quadrature current, i_{qs}^*, is computed from the torque command. The direct current, i_{ds}^*, is computed from the rotor flux. These dq currents are transformed to the reference three phase currents. Current sensors measure the actual phase currents which sent to the DS1104 platform via analog to digital converters. The actual and reference currents are compared using hysteresis comparators to give the six pulses of the six IGBT's switches. Fig. 7 depicts a picture of the real-time experimental system for IM drive system via DSP-DS1104 platform. Traditional 1DOF and 2DOF approaches as well as the proposed VSC approach are implemented using the IFOC of the IM drive.

B. Simulation and Experimental Tests

The simulation model of the proposed controller for an IM drive is built on Matlab/Simulink. Also, a laboratory prototype of IM drive is executed in the laboratory. The proposed VSC approach is implemented and compared with the classic control schemes during step speed variation and load torque disturbance. Different tests demonstrating the behavior of the proposed VSC approach in comparison to classic control approaches are provided.

Simulation and experimental responses of the reference and actual speeds under step speed change using 1DOF control method are illustrated in Fig. 8(a) and Fig. 8(b), respectively. It is noted that the speed response has a large overshoot, undershoot, and large settling time (around 0.26 sec).

To test the 1DOF control scheme under load torque disturbance, Fig. 9 (a and b) demonstrates the simulation and experimental responses during step load change using 1DOF control method. It is seen that the speed dip is high with a value of 0.015 p.u (9.33 %). Moreover, there is a big recovery time that reached to 0.2 sec.

The performance of the 2DOF control scheme is tested at the same conditions of 1DOF control scheme. Figs. 10 and 11 show the simulation and experimental responses of the reference and actual speeds using 2DOF control method under step speed change and step load change, respectively. It is found that the speed response under step speed change is enhanced. It has smaller overshoot and settling time than the corresponding ones using 1DOF scheme. However, the speed response under step load change with 2DOF control method is the same as 1DOF scheme.

To validate the efficacy of the proposed VSC approach in comparison to the classic control methods (1DOF and 2DOF), Figs. 12 and 13 show the results at similar conditions. It is obvious that the speed response has a good tracking performance without overshoot and undershoots. The rise and settling times are smaller than the corresponding ones using the classic control methods (1DOF and 2DOF). Furthermore, the speed dip and the recovery time under load torque change prove the good load torque rejection.

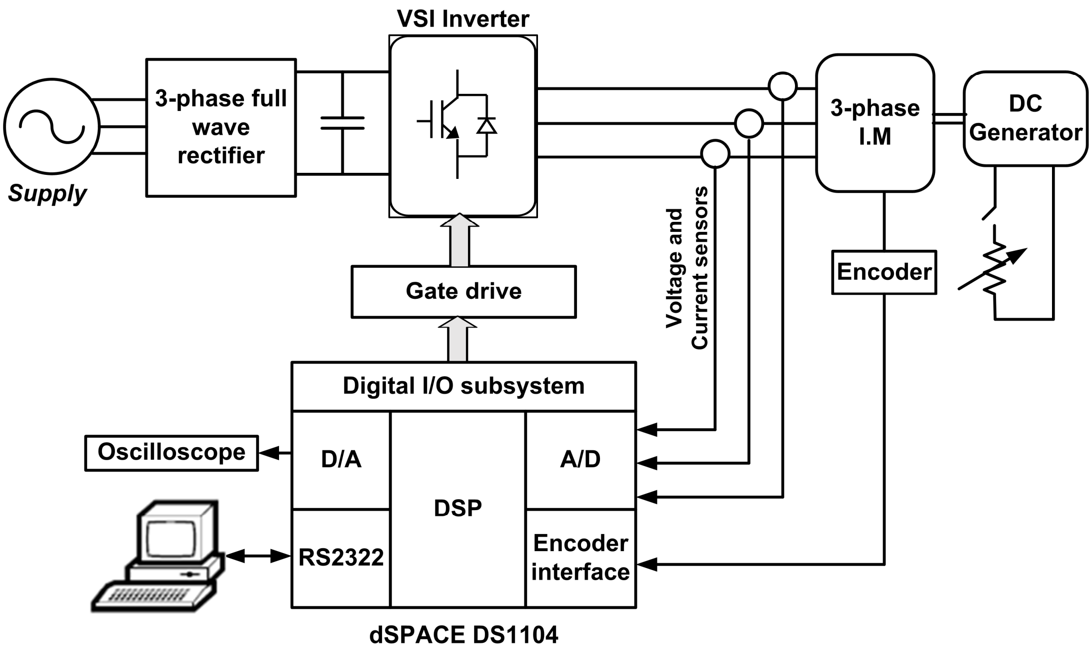

Figure 6. Experimental layout for IM drive system using DSP-DS1104 control platform

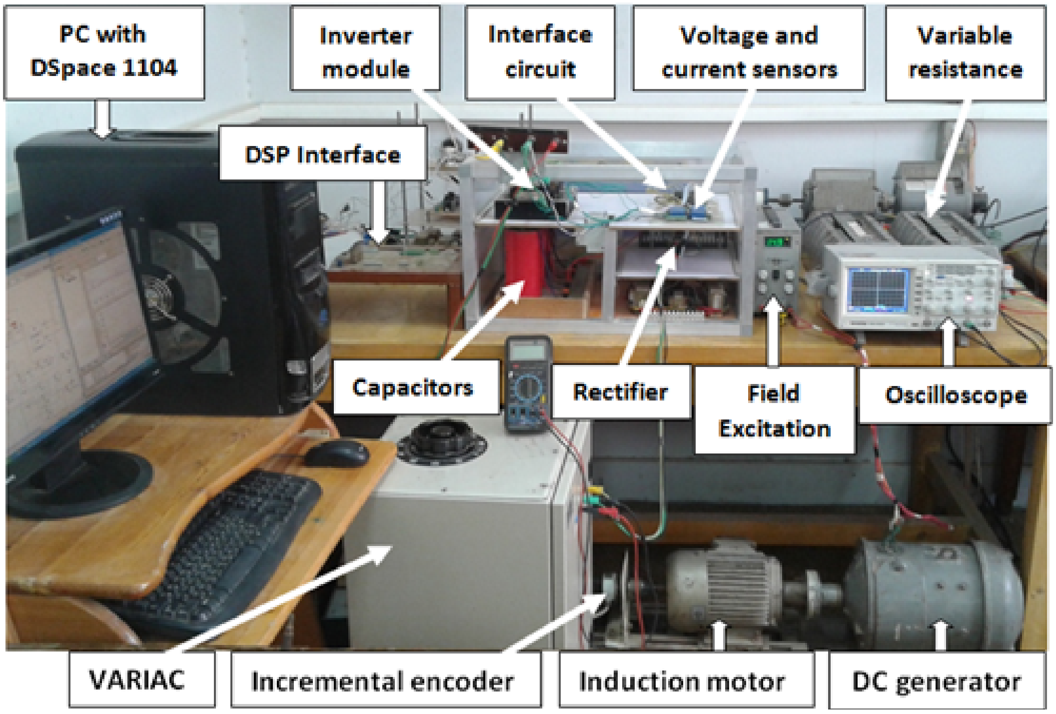

Figure 7. Picture of the real-time experimental system for IM drive with DSP-DS1104 control platform

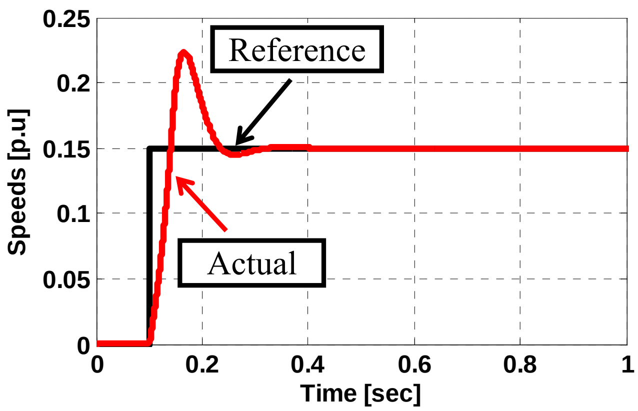

(a)

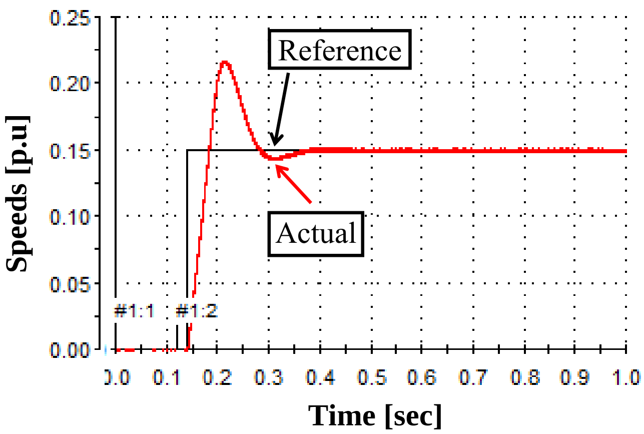

(b)

Figure 8. Responses of the reference and actual speeds under step speed change using 1DOF control method. (a) Simulation. (b) Experimental

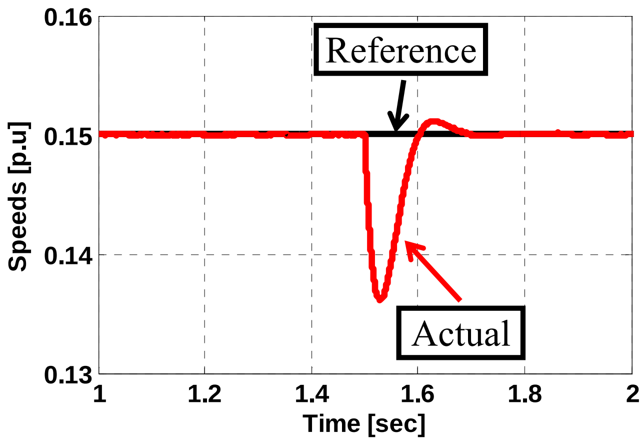

(a)

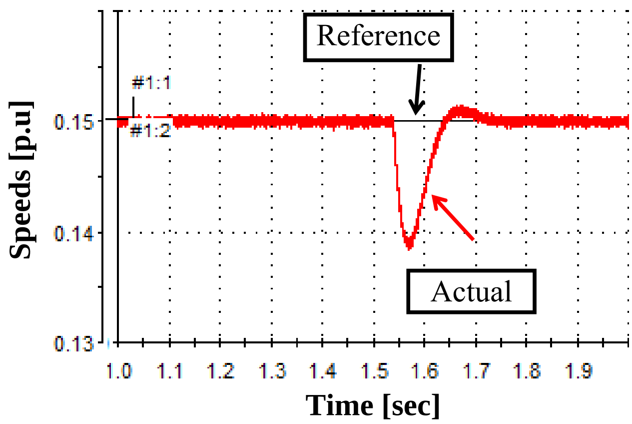

(b)

Figure 9. Responses of the reference and actual speeds under step load change using 1DOF control method. (a) Simulation. (b) Experimental

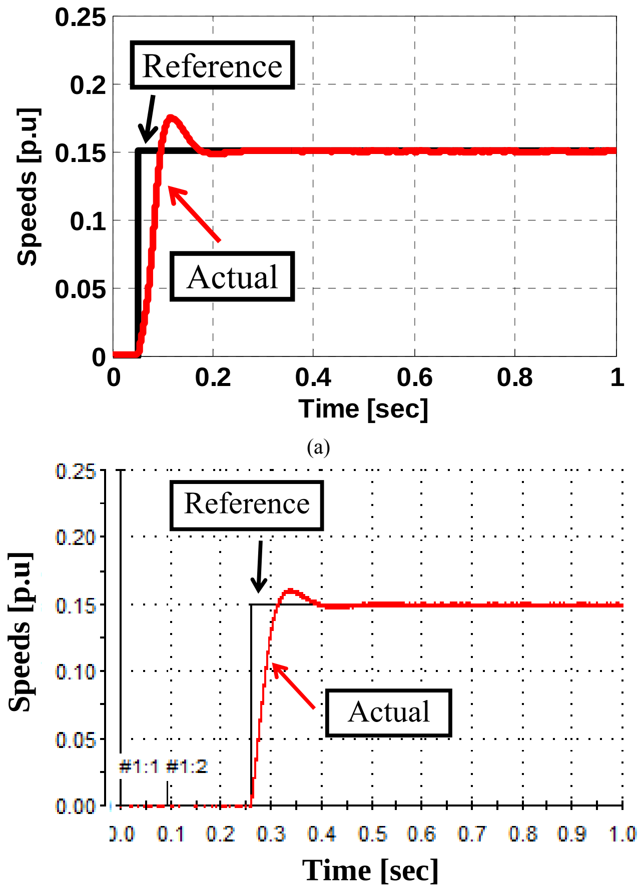

(b)

Figure 10. Responses of the reference and actual speeds under step speed change using 2DOF control method. (a) Simulation. (b) Experimental

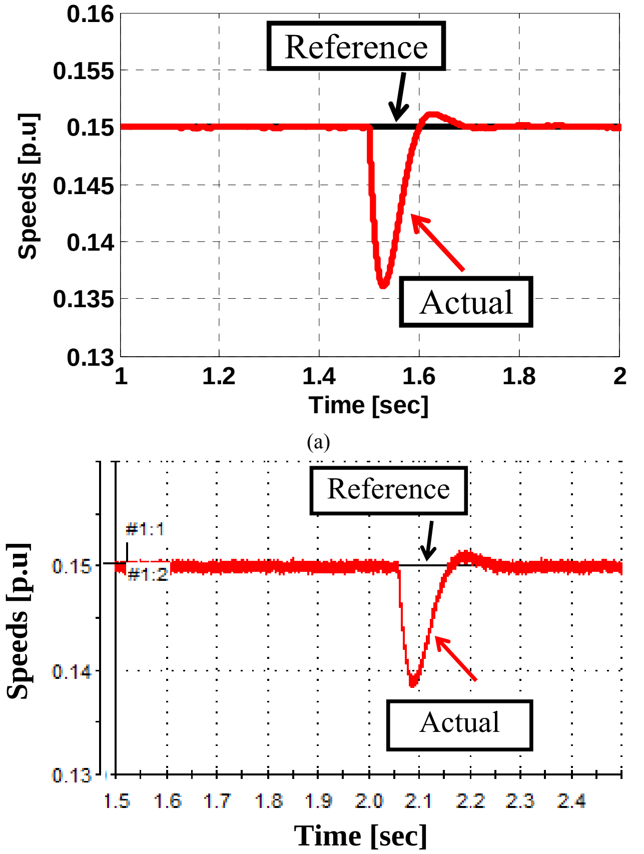

(b)

Figure 11. Responses of the reference and actual speeds under step load change using 2DOF control method. (a) Simulation. (b) Experimental

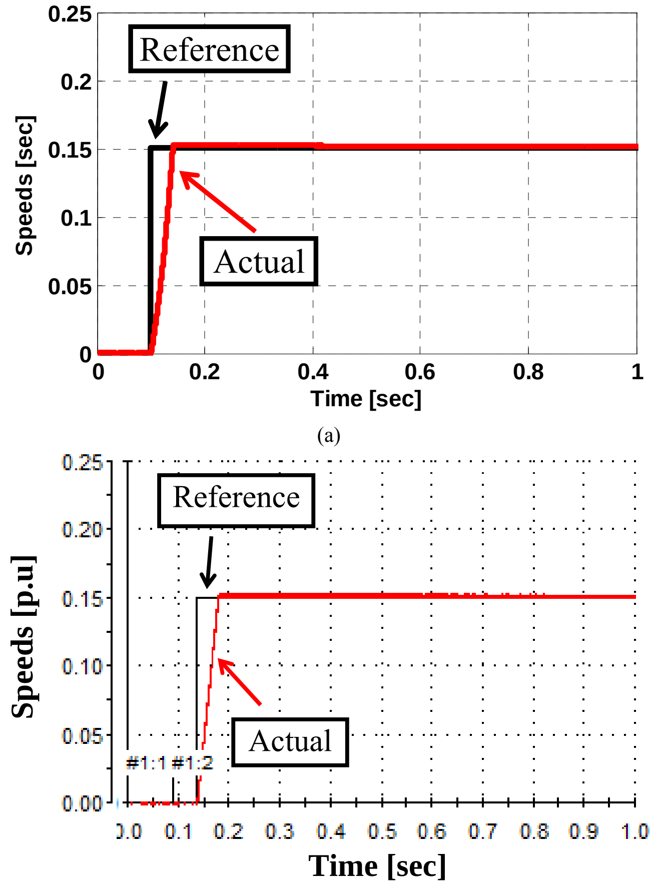

(b)

Figure 12. Responses of the reference and actual speeds under step speed change using VSC control method. (a) Simulation. (b) Experimental

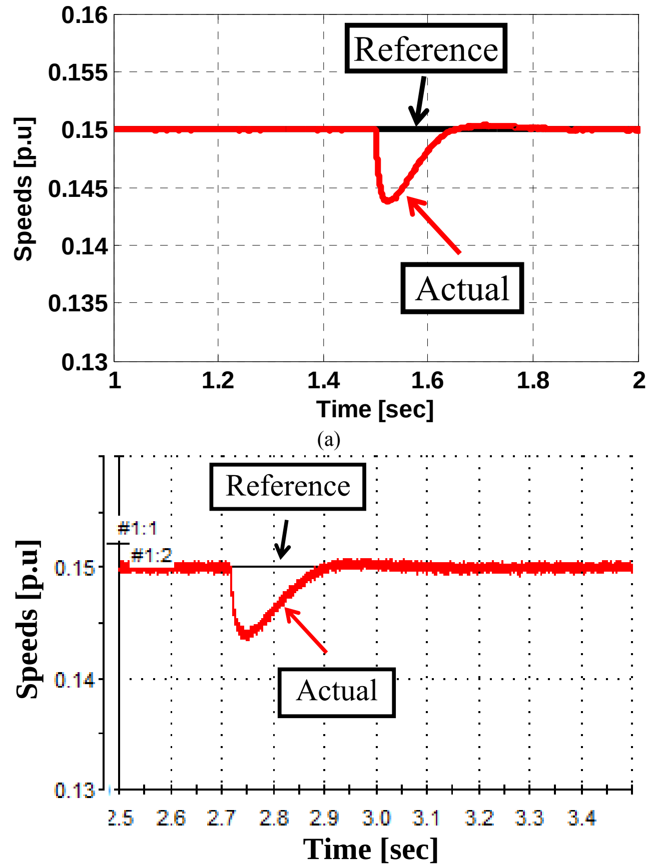

(b)

Figure 13. Responses of the reference and actual speeds under step load change using VSC control method. (a) Simulation. (b) Experimental

VII. RESULTS COMPARISON

Table II illustrates the quantitative behavior comparison of the suggested VSC algorithm with classic 1DOF and 2DOF control schemes. It is evident that the proposed VSC approach has a significant performance compared to the classic controllers. It has a smaller rise and settling times than the corresponding ones with the classic controllers. Also, it has not an overshoot. Moreover, it has a small dip speed with low recovery time under load torque disturbances. As noted, the suppression of the disturbances is much improved compared to the classic control methods (1DOF and 2DOF).

Table II. QUANTITATIVE BEHAVIOR COMPARISON OF THE PROPOSED TECHNIQUE WITH PREVIOUS CONTROLLERS.

Method	**Performance Indicators**				
	Speed Reference Tracking			Load Torque Disturbance	
	Rise Time	Settling Time	Overshoot	Speed Dip	Recovery Time
1DOF [32]	0.05 sec	0.26 sec	46.6%	9.33%	0.2 sec
2DOF [32]	0.04 sec	0.14 sec	13.33%	8%	0.2 sec
Proposed VSC	0.03 sec	0.05 sec	0%	4%	0.18 sec

VIII. CONCLUSION

In this paper, the dynamic response of the IM drive under the reference tracking and the load disturbance has been improved using the proposed VSC scheme. The designed controller incorporates the two advantages of VSC and 2DOF schemes. The obtained results proved that the traditional 1DOF controller can not satisfy the desired performance under the reference tracking and the load disturbance. It has overshoot, undershoot, and large settling time under speed reference change. Moreover, large speed dip with large recovery time to reach the steady state was observed under torque change. The 2DOF controller improves the performance under step speed change compared to 1DOF controller. However, the suppression of the disturbances cannot be fully achieved. Alternatively, the disturbances using the proposed VSC scheme are strongly suppressed compared to only 2DOF scheme. It has a rapid response with zero steady state error without overshoot and undershoot. Also, it has a low speed dip with small recovery time under load torque disturbance.

APPENDIX

TABLE I. PARAMETERS OF IM

Rated power	1.1 kW	R_s	7.4826 ohm
Supply voltage	380 volts	R_r	3.6840 ohm
Rated current	2.545 Amp	L_r	0.0221 H
No. of poles	4	L_s	0.0221 H
Supply frequency	50 Hz	L_m	0.4114 H
		J	0.02 kg.m^2

REFERENCES

[1] S. Jikai, F. Haichao, A. Liwang, H. Yihua, C. Wenping, "Design and Analysis of a 2-DOF Split-Stator Induction Motor," IEEE Transactions on Energy Conversion, vol. 30, Issue 3, pp. 1200–1208, 2015. doi:10.1109/TEC.2015.2418578

[2] S. Jikai, A. Liwang, F. Haichao, Z. Yifeng, H. Yihua, "Analysis on coupling effect of 2-DOF direct drive induction motor based on 3-D model," 17th International Conference on Electrical Machines and Systems (ICEMS), pp. 1157–1163, 2014. doi:10.1109/ICEMS.2014.7013653

[3] M. Caruso, V. Cecconi, V. Di Dio, A. O. Di Tommaso, F. Genduso, D. La Cascia, R. Liga, R. Miceli, " Speed control of a two-degrees of freedom induction motor with rotor Helical Motion for industrial applications", AEIT Annual Conference - From Research to Industry: The Need for a More Effective Technology Transfer (AEIT), pp. 1–6, 2014. doi:10.1109/AEIT.2014.7002051

[4] D. Campos-Gaona; E.L. Moreno-Goytia; O. Anaya-Lara, "Fault Ride-Through Improvement of DFIG-WT by Integrating a Two-Degrees-of-Freedom Internal Model Control", IEEE Transactions on Industrial Electronics, vol. 60, issue: 3, pp. 1133–1145, 2013. doi:10.1109/TIE.2012.2216234

[5] F. M. El-Sousy, "Design and implementation of 2DOF I-PD controller for indirect field orientation control induction machine drive system", Proceedings of IEEE International Symposium on Industrial Electronics , ISIE 2001, Pusan, South Korea, vol. 2, pp. 1112-1118, 2001. doi:10.1109/ISIE.2001.931632

[6] S. Brock, D. Łuczak, K. Nowopolski, T. Pajchrowski, K. Zawirski," Two Approaches to Speed Control for Multi-Mass System With Variable Mechanical Parameters", IEEE Transactions on Industrial Electronics, vol. 64, issue 4, pp. 3338–3347, 2017. doi:10.1109/TIE.2016.2598299

[7] I. A. Ivan, F. Ahmad, J. Agnus, P. Lutz, M. Rakotondrabe," Quasi-static displacement self-sensing measurement for a 2-DOF piezoelectric cantilevered actuator" IEEE Transactions on Industrial Electronics, vol. 64, issue 8, pp. 6330 - 6337, 2017. doi:10.1109/TIE.2017.2677304

[8] M. R. Soltanpour; P. Otadolajam, M. H. Khooban, "Robust control strategy for electrically driven robot manipulators: adaptive fuzzy sliding mode", IET Science, Measurement & Technology, vol. 9, issue 3, pp. 322 – 334, 2015. doi:10.1049/iet-smt.2013.0265

[9] R.J. Caverly, J.R. Forbes, "Dynamic Modeling and Noncollocated Control of a Flexible Planar Cable-Driven Manipulator", IEEE Transactions on Robotics, vol. 30, Issue 6, pp. 1386–1397, 2014. doi:10.1109/TRO.2014.2347573

[10] J. W. Wu, J. J. Chen; M. L. Chiang; J. T Yu; L. C. Fu, " Design and Control of Phase-Detection Mode Atomic Force Microscopy for Reconstruction of Cell Contours in Three Dimensions", IEEE Transactions on Nanotechnology, vol. 13, issue: 4, pp. 639–649, 2014. doi:10.1109/TNANO.2014.2307073

[11] L. Zhou, Y. Chen, A. Luo, J. M. Guerrero, X. Zhou, Z. Chen, W. Wu, "Robust two degrees-of-freedom single-current control strategy for LCL-type grid-connected DG system under grid-frequency fluctuation and grid-impedance variation", IET Power Electronics, vol. 9, issue 14, pp. 2682 – 2691, Year: 2016. doi:10.1049/iet-pel.2016.0120

[12] T. J. Teo, H. Zhu, C.K. Pang, "Modeling of a Two Degrees-of-Freedom Moving Magnet Linear Motor for Magnetically Levitated Positioners", IEEE Transactions on Magnetics, vol. 50, issue 12, 2014. doi:10.1109/TMAG.2014.2341646

[13] Y. Sato, K. Murakami, Y. Tsuboi, "Sensorless Torque and Thrust Estimation of a Rotational/Linear Two Degrees-of-Freedom Switched Reluctance Motor", IEEE Transactions on Magnetics, vol. 52, issue 7, 2016. doi:10.1109/TMAG.2016.2536682

[14] E.W. Hawkes, D.L. Christensen, M.T. Pope, M.R. Cutkosky, "One Motor, Two Degrees of Freedom Through Dynamic Response Switching", IEEE Robotics and Automation Letters, vol. 1, issue 2, pp. 969 – 975, 2016. doi:10.1109/LRA.2016.2526066

[15] M. Seilmeier, B. Piepenbreier, "Sensorless Control of PMSM for the Whole Speed Range Using Two-Degree-of-Freedom Current Control and HF Test Current Injection for Low-Speed Range", IEEE Transactions on Power Electronics, vol. 30, issue 8, pp. 4394–4403, 2015. doi:10.1109/TPEL.2014.2353215

[16] M. S. Zaky, A self-tuning PI controller for the speed control of electrical motor drives, Electr. Pow. Syst. Res., vol. 119, pp. 293–303 2015. doi:10.1016/j.epsr.2014.10.004

[17] M. S. Zaky, "Robust chatter-free continuous VSC for the speed control of electrical motor drives using adaptive feedback gain", Electric Power Systems Research, vol. 140, pp. 786–796, 2016. doi:10.1016/j.epsr.2016.05.007

[18] M. Zaky, E. Elattar, M. Metwaly, "Decoupled Speed and Torque Control of IPMSM Drives Using a Novel Load Torque Estimator," Advances in Electrical and Computer Engineering, vol. 17, No. 3, pp. 19-28, 2017. doi:10.4316/AECE.2017.03003

[19] Q. C. Zhong and J. E. Normey-Rico, "Control of integral processes with dead-time. Part 1. Disturbance observer-based 2 DOF control scheme, IEE Proceedings - Control Theory and Applications, vol. 149, no. 4, pp. 285-290, 2002. doi:10.1049/ip-cta:20020438

[20] Radu-Emil Precup and Stefan Preitl, "PI and PID controllers tuning for integral-type servo systems to ensure robust stability and

controller robustness, Electrical Engineering, vol. 88, no. 2, pp. 149-156, 2006. doi:10.1007/s00202-004-0269-8

[21] Saurabh Srivastava, V. S. Pandit, "A 2-Dof LQR based PID controller for integrating processes considering robustness/performance tradeoff, ISA Transactions, vol. 71, part 2, pp. 426-439, 2017. doi:10.1016/j.isatra.2017.09.010

[22] P. A. Egiguren, O. B. Caramazana; I. G. Hernandez; A. J. Hernandez "Robust adaptive Variable Structure Control of induction motor drives." IEEE International Symposium on Industrial Electronics, ISIE, 2008, pp. 582 – 587. doi:10.1109/ISIE.2008.4676940

[23] J. Hung, W. Gao, and J. Hung, "Variable Structure Control: A Survey," IEEE Trans. on Ind. Electronics, vol. 40, no. 1, pp 2-22, 1993. doi:10.1109/41.184817

[24] M. Zaky, S. Shaban, T. Fetouh, "Adaptive and Robust Sliding Mode Position Control of IPMSM Drives," Advances in Electrical and Computer Engineering, vol. 17, no. 1, pp. 61-68, 2017. doi:10.4316/AECE.2017.01009

[25] O. Barambones, A. J. Garrido, F. J. Maseda, " Integral sliding-mode controller for induction motor based on field-oriented control theory," IET Control Theory & Applications, vol. 1, no. 3, pp. 786-794, 2007. doi:10.1049/iet-cta:20060239

[26] V. I. Utkin, "Sliding mode control design principles and applications to electric drives," IEEE Trans. Ind. Electron., vol. 40, pp. 26–36, 1993. doi:10.1109/41.184818

[27] A. Leon-Masich, H. Valderrama-Blavi, J. M. Bosque-Moncusí, J. Maixé-Altés, and L. Martínez-Salamero, "Sliding-mode-control-based boost converter for high-voltage-low-power applications, IEEE Transactions on Industrial Electronics, vol. 62, no. 1, pp. 229-237, 2015. doi:10.1109/TIE.2014.2327004

[28] S. Biricik, and H. Komurcugil, "Optimized sliding mode control to maximize existence region for single-phase dynamic voltage restorers, IEEE Transactions on Industrial Informatics, vol. 12, no. 4, pp. 1486-1497, 2016. doi:10.1109/TII.2016.2587769

[29] A. Pisano, M. Tanelli, A. Ferrara, "Switched/time-based adaptation for second-order sliding mode control, Automatica, vol. 64, pp. 126-132, 2016. doi:10.1016/j.automatica.2015.11.006

[30] Radu-Emil Precup, Mircea-Bogdan Radac, Raul-Cristian Roman, Emil M. Petriu, "Model-free sliding mode control of nonlinear systems: Algorithms and experiments, Information Sciences, vol. 381, pp. 176-192, 2017. doi:10.1016/j.ins.2016.11.026

[31] S. K. Chung, J. H. Lee, J.S. KO, M.J.Youn, "Robust speed control of brushless direct-drive motor using integral variable structure control," IEE Proc.-Electr. Power Appl, vol. 142, no. 6, pp. 361-370, November 1995. doi:10.1049/ip-epa:19952230

[32] L. Harnefors, S. E. Saarakkala, and M. Hinkkanen, Speed Control of Electrical Drives Using Classical Control Methods, IEEE Transactions on Industry Applications, vol. 49, no. 2, pp. 889-898, 2013. doi:10.1109/TIA.2013.2244194